Benchmark calculations of chemical reactions in density functional theory: comparison of the accurate Kohn-Sham solution with generalized gradient approximations for the H2+H and H2+H2 reactions.

Schipper, P.R.T.; Gritsenko, O.V.; Baerends, E.J.

published in
Journal of Chemical Physics
1999

DOI (link to publisher)
10.1063/1.479707

document version
Publisher's PDF, also known as Version of record

Benchmark calculations of chemical reactions in density functional theory: Comparison of the accurate Kohn–Sham solution with generalized gradient approximations for the H_2+H and H_2+H_2 reactions

P. R. T. Schipper, O. V. Gritsenko, and E. J. Baerends
Scheikundig Laboratorium der Vrije Universiteit, De Boelelaan 1083, 1081 HV Amsterdam, The Netherlands

(Received 11 February 1999; accepted 9 June 1999)

The Kohn–Sham (KS) solution is constructed from an accurate CI density and the KS exchange and correlation energies E_x and E_c, as well as the corresponding exchange and exchange-correlation energy densities $\epsilon_x(\mathbf{r})$ and $\epsilon_{xc}(\mathbf{r})$, which are obtained for the hydrogen abstraction reaction $H+H_2$ and the symmetrical four-center exchange reaction H_2+H_2. The KS quantities are compared with those of the standard GGAs. Comparison shows that the GGA exchange functional represents both exchange and molecular nondynamical left–right correlation, while the GGA correlation functional represents only the dynamical part of the correlation. This role of the GGA exchange functional is especially important for the transition states (TS) of the reactions where the left–right correlation is enhanced. Standard GGAs tend to underestimate the barrier height for the reaction $H+H_2$ and to overestimate it for the reaction H_2+H_2. For H_2+H_2 the Kohn–Sham orbital degeneracy in the square TS is represented with an equi-ensemble KS solution for both accurate KS/CI and GGA, while near the TS ensemble solutions with unequal occupations of the degenerate highest occupied orbitals are obtained. For the GGA ensemble solution a special ensemble formula for the GGA exchange functional is proposed. Application of this formula to the H_2+H_2 reaction reduces appreciably the reaction barriers calculated with GGAs and leads to much better agreement with the accurate value. The too low GGA barriers for the $H+H_2$ reaction are attributed to overestimation of the dynamical correlation in the TS by the GGA correlation functionals. In order to correct this error, it is recommended to modify the dependence of the approximate correlation functionals on the local polarization ζ with the purpose of reducing the approximate correlation energy for intermediate ζ values, which are expected to characterize the TS's of radical abstraction reactions.
 [S0021-9606(99)30733-9]

I. INTRODUCTION

With the advent of the generalized gradient approximations (GGAs),[1–4] density functional theory (DFT) has become a powerful tool for computational chemistry. GGAs are successfully applied to the calculation of various molecular properties such as atomization energies and equilibrium geometries. However, the quality of the GGA calculations of potential energy surfaces of chemical reactions appears to be nonuniform. For certain types of reactions, most notably for the hydrogen abstraction reactions, it was established in the literature that the standard GGAs yield too low reaction barriers.[5–8] None of these studies compares GGAs with the essentially accurate Kohn–Sham (KS) solution, which can be obtained from an accurate *ab initio* electron density $\rho(\mathbf{r})$. Previously, such solutions have been obtained for a number of atoms[9–12] and molecules.[13–20]

In this paper the KS solution is constructed from an *ab initio* ρ and the KS exchange and correlation energies E_x and E_c, as well as the corresponding exchange and exchange-correlation energy densities $\epsilon_x(\mathbf{r})$ and $\epsilon_{xc}(\mathbf{r})$, are calculated for a number of points [including the transition state (TS)] along the paths of the simplest collinear hydrogen abstraction reaction $H+H_2$ and the symmetry-forbidden four-center exchange reaction H_2+H_2. The *ab initio* densities have been obtained with high quality configuration interaction (CI) calculations at many points of the two-dimensional potential energy surface (PES) of the symmetrical H_2+H_2 reaction and the collinear path of the $H+H_2$ reactions. In Sec. II the computational details are discussed and the method of construction of the KS solution is characterized.

In Sec. III the PES for the reaction H_2+H_2 is presented and the construction of the KS solution around the square TS of D_{4h} symmetry is discussed. In this region the proper KS and GGA solutions are represented with an ensemble of degenerate determinants similar to the case of the C_2 molecule considered in our previous paper.[18] In Sec. IV the CI results and the accurate KS exchange and correlation energy densities for the reaction H_2+H_2 are compared with those of GGAs. The standard GGAs appreciably overestimate the reaction barrier. It is proposed to use for the GGA ensemble solution around the TS a special ensemble formula for E_x. Application of this formula reduces the reaction barriers calculated with GGAs and leads to much better agreement with the accurate value. In Sec. V the CI results and the KS exchange and correlation energy densities for the reaction $H+H_2$ are compared with the GGA ones. In agreement with previous studies, GGAs are found to underestimate the barrier of this reaction. To improve the performance of the GGA

for $H+H_2$ without worsening its results for H_2+H_2, it is proposed to modify the spin-polarization dependence of the GGA correlation energy functional in order to reduce the Coulomb correlation of the electrons with like spins, which is overestimated by the GGA. In Sec. VI conclusions are drawn. One conclusion is that, owing to its localized model Fermi hole, the GGA exchange functional represents effectively both exchange and molecular left–right nondynamical correlation. The GGA correlation functional, in its turn, represents only the dynamical short-range correlation. The same trend has been observed in our previous work for diatomic molecules Li_2, N_2, F_2,[16,17] and for H_2.[21,22] Comparison of the KS and GGA energy densities $\epsilon_x(\mathbf{r})$ and $\epsilon_{xc}(\mathbf{r})$ supports this conclusion.

II. CALCULATION OF THE KS QUANTITIES

The iterative procedure used in this paper to obtain the Kohn–Sham orbitals $\psi_i(\mathbf{r})$ and potential $v_s(\mathbf{r})$ from an *ab initio* density $\rho(\mathbf{r})$ has been developed recently in Ref. 23. It starts from a trial potential $v_s^0(\mathbf{r})$:

$$v_s^0(\mathbf{r})=v_{\text{ext}}(\mathbf{r})+v_H(\mathbf{r})+v_{X\alpha}(\rho;\mathbf{r})+2\epsilon_{x,nl}^B(\rho,|\nabla\rho|;\mathbf{r}) +2\epsilon_c^{\text{VWN}}(\rho;\mathbf{r}), \tag{2.1}$$

which produces the starting density $\rho^0(\mathbf{r})$ built from the orbitals $\psi_i^0(\mathbf{r})$. In Eq. (2.1) $v_{\text{ext}}(\mathbf{r})$ is the external potential of the nuclei, $v_H(\mathbf{r})$ is the Hartree potential of the electrostatic electron repulsion calculated with a suitable initial density, $v_{X\alpha}(\mathbf{r})$ is the exchange-correlation $X\alpha$ potential,[24] $\epsilon_{x,nl}^B$ is the exchange energy density gradient correction of Becke,[3] and ϵ_c^{VWN} is the local density approximation (LDA) of Vosko, Wilk and Nusair[25] for the correlation energy. At the $n+1$-th iteration a change of the potential $\delta v_s^n(\mathbf{r})=v_s^{n+1}(\mathbf{r})-v_s^n(\mathbf{r})$ is calculated using the total $\rho^n(\mathbf{r})$ and orbital $\rho_i^n(\mathbf{r})=f_i|\psi_i^n(\mathbf{r})|^2$ densities obtained at the previous iteration as well as the target $\rho(\mathbf{r})$:

$$\delta v_s^n(\mathbf{r})=\frac{1}{4\rho^n(\mathbf{r})}\left\{\nabla^2\rho(\mathbf{r})-\frac{\rho(\mathbf{r})}{\rho^n(\mathbf{r})}\nabla^2\rho^n(\mathbf{r}) -\frac{1}{\rho^n(\mathbf{r})}\left(\nabla\rho(\mathbf{r})\cdot\nabla\rho^n(\mathbf{r})-\frac{\rho(\mathbf{r})}{\rho^n(\mathbf{r})}\left|\nabla\rho^n(\mathbf{r})\right|^2\right)\right\} +\sum_{i=1}^{N-1}\delta v_{si}^n\frac{\rho_i^n(\mathbf{r})}{\rho^n(\mathbf{r})}, \tag{2.2}$$

where $\delta v_{si}^n=\langle\psi_i^n|\delta v_s^n|\psi_i^n\rangle$, the diagonal matrix elements of δv_s^n, are calculated from a set of independent linear equations

$$\sum_{i=1}^{N}\left(\int\frac{\rho_j^n(\mathbf{r})\rho_i^n(\mathbf{r})}{\rho^n(\mathbf{r})}d\mathbf{r}-f_j\delta_{ji}-f_i\delta_{iN}\right)\delta v_{si}^n =-\int\frac{\rho_j^n(\mathbf{r})}{4\rho^n(\mathbf{r})}\left\{\nabla^2[\rho(\mathbf{r})-\rho^n(\mathbf{r})] -\nabla\cdot\left(\frac{[\rho(\mathbf{r})-\rho^n(\mathbf{r})]\nabla\rho^n(\mathbf{r})}{\rho^n(\mathbf{r})}\right)\right\}d\mathbf{r}. \tag{2.3}$$

To derive Eqs. (2.2),(2.3), the response of the KS orbitals to the potential change δv_s is considered within linear response theory and an approximation for the orbital density response $\delta\rho_i(\mathbf{r})\approx\delta\rho(\mathbf{r})\rho_i(\mathbf{r})/\rho(\mathbf{r})$ is employed.[23] An updated potential $v_s^{n+1}(\mathbf{r})=v_s^n(\mathbf{r})+\delta v_s^n(\mathbf{r})$ is used to calculate a new set of orbitals $\psi_i^{n+1}(\mathbf{r})$ and the iterative procedure continues until convergence is reached. The accuracy of the resultant KS solution can be characterized by the values of the absolute integral error $\Delta\rho$ for the calculated density $\rho^m(\mathbf{r})$

$$\Delta\rho=\int|\rho^m(\mathbf{r})-\rho(\mathbf{r})|d\mathbf{r}. \tag{2.4}$$

The magnitude of ρ depends on the quality of the target *ab initio* ρ as well as on the system considered. For the most accurate target densities, typical errors are small, with the maximal errors being only $\Delta\rho=0.0002e$ for the H_3 TS and $\Delta\rho=0.001e$ for the H_4 TS. In general, the procedure of Eqs. (2.1)–(2.3) provides a higher accuracy of the KS solution with fewer iterations compared to that of van Leeuwen and Baerends[26] employed in our previous work.

To obtain *ab initio* correlated wave functions and densities, the HF and subsequent CI calculations of the two-dimensional PES of the H_2+H_2 reaction and the collinear $H+H_2$ reaction have been performed by means of the ATMOL package.[27] A basis of contracted Gaussian functions has been used for the calculations. A high quality quintuple zeta basis set (cc-pV5Z)[28] has been used for a number of points along the reaction paths. For the larger H_2+H_2 system the *g*-type polarization function has been omitted from the basis and two *f*-type functions have been replaced with one *f*-function taken from the quadruple cc-pVQZ basis. The extensive multireference CI (MRCI) calculations have been carried out within the direct CI approach with the reference configurations produced by the inclusion of all excitations in an internal space of 24 orbitals. All single and double excitations from each reference configuration have been included in the MRCI. For the bulk of the calculations for the PES a smaller (though also large enough) augmented triple zeta (aug-cc-pVTZ) basis has been used. In this case the single reference CI calculations have been carried out with all single and double excitations from the HF configuration. The high quality of our CI calculations can be illustrated by the fact that they yield as barrier height of the hydrogen abstraction reaction $E^B=9.64$ kcal/mol, which is even closer to the experimental value $E_{\text{exp}}^B=9.7$ kcal/mol[5,29] than a high-quality quantum Monte Carlo result of 9.61 kcal/mol.[5,30]

The Kohn–Sham exchange energy density $\epsilon_x(\mathbf{r}_1)$ has been calculated according to the conventional expression

$$\epsilon_x(\mathbf{r}_1)=-\frac{1}{2\rho(\mathbf{r}_1)}\sum_{i=1}^{N}\sum_{j=1}^{N}\int d\mathbf{r}_2 \times\frac{\psi_i^*(\mathbf{r}_1)\psi_j(\mathbf{r}_1)\psi_j^*(\mathbf{r}_2)\psi_i(\mathbf{r}_2)}{|\mathbf{r}_1-\mathbf{r}_2|} \tag{2.5}$$

from the KS orbitals $\psi_i(\mathbf{r})$ obtained with the iterative procedure Eqs. (2.1)–(2.3). The KS exchange-correlation energy density $\epsilon_{xc}(\mathbf{r}_1)$ is defined according to Refs. 21, 31 as the sum

$$\epsilon_{xc}([\rho];\mathbf{r})=v_{c,\text{kin}}([\rho];\mathbf{r})+\tfrac{1}{2}v_{xc}^{\text{hole}}([\rho];\mathbf{r}) \tag{2.6}$$

of the potential of the exchange-correlation hole v_{xc}^{hole}

$$v_{xc}^{\text{hole}}(\mathbf{r}) = \int \frac{\rho_2(\mathbf{r}_1,\mathbf{r}_2) - \rho(\mathbf{r}_1)\rho(\mathbf{r}_2)}{|\mathbf{r}_1 - \mathbf{r}_2|\rho(\mathbf{r}_1)} d\mathbf{r}_2 \tag{2.7}$$

and the kinetic part $v_{c,\text{kin}}$

$$v_{c,\text{kin}}(\mathbf{r}_1) = \frac{\nabla_{1'}\nabla_1[\rho(\mathbf{r}_1',\mathbf{r}_1) - \rho_s(\mathbf{r}_1',\mathbf{r}_1)]|_{\mathbf{r}_1'=\mathbf{r}_1}}{2\rho(\mathbf{r}_1)}. \tag{2.8}$$

To construct $\epsilon_{xc}(\mathbf{r}_1)$ via Eqs. (2.6)–(2.8), the first-order density matrix $\rho(\mathbf{r}_1',\mathbf{r}_1)$ and the diagonal part $\rho_2(\mathbf{r}_1,\mathbf{r}_2)$ of the two-electron density matrix have been calculated from the MRCI wave function by means of a Gaussian orbital density functional code[13,32] based on the ATMOL package. The KS first-order density matrix $\rho_s(\mathbf{r}_1',\mathbf{r}_1)$ in Eq. (2.8) has been calculated from the orbitals $\psi_i(\mathbf{r})$.

The GGA functionals considered in this paper are the exchange-correlation functional of Perdew and Wang (PW 91),[4,33,34] the combination BP of the exchange functional of Becke[3] and the correlation functional of Perdew (P86)[1] and the combination of the same exchange functional of Becke with the correlation functional of Lee, Yang, and Parr (LYP).[2] The GGA calculations have been performed both self-consistently and with the CI $\rho(\mathbf{r})$. The GGA exchange ϵ_x^{GGA} and exchange-correlation $\epsilon_{xc}^{\text{GGA}}$ energy densities define according to the expressions

$$E_x^{\text{GGA}}[\rho] = \int \rho(\mathbf{r})\epsilon_x^{\text{GGA}}([\rho];\mathbf{r})d\mathbf{r}, \tag{2.9}$$

$$E_{xc}^{\text{GGA}}[\rho] = \int \rho(\mathbf{r})\epsilon_{xc}^{\text{GGA}}([\rho];\mathbf{r})d\mathbf{r}, \tag{2.10}$$

the corresponding exchange E_x^{GGA} and exchange-correlation E_{xc}^{GGA} energies. In this paper the accurate KS energy densities Eqs. (2.5) and (2.6) are compared with the GGA ones calculated with the CI $\rho(\mathbf{r})$. In particular, for the open-shell $H+H_2$ system the total GGA exchange energy density $\epsilon_x^{\text{GGA}}(\rho^\uparrow,\rho^\downarrow;\mathbf{r})$ has been calculated from the CI spin-densities $\rho^\uparrow(\mathbf{r})$ and $\rho^\downarrow(\mathbf{r})$ as follows:

$$\epsilon_x^{\text{GGA}}(\rho^\uparrow,\rho^\downarrow;\mathbf{r}) = \frac{\rho^\uparrow(\mathbf{r})\epsilon_x^{\text{GGA}}(\rho^\uparrow;\mathbf{r}) + \rho^\downarrow(\mathbf{r})\epsilon_x^{\text{GGA}}(\rho^\downarrow;\mathbf{r})}{\rho(\mathbf{r})}. \tag{2.11}$$

III. POTENTIAL ENERGY SURFACE AND THE ENSEMBLE SOLUTION FOR THE TS OF THE H_2+H_2 REACTION

Figure 1 presents the two-dimensional PES from a CI calculation for the symmetry-forbidden four-center exchange reaction H_2+H_2. Each point of the figure corresponds to a rectangle H_4 with sides x and y, so that $r=\min(x,y)$ is the bond distance in each H_2 fragment and $R=\max(x,y)$ is the distance between the fragments. Along the reaction path, for the larger intermolecular separations $R>3.0$ a.u. the bond distance r in each H_2 is close to its equilibrium value $r=1.4$ a.u. for the individual H_2 molecule. For the shorter separations r gradually increases until the system reaches the square transition state (TS) with $r=R=2.32$ a.u. This produces a monotonous increase of the total energy and a high reaction barrier $E^B=147.6$ kcal/mol. The TS is unstable with respect to dissociation into a H_2 molecule and two H atoms,

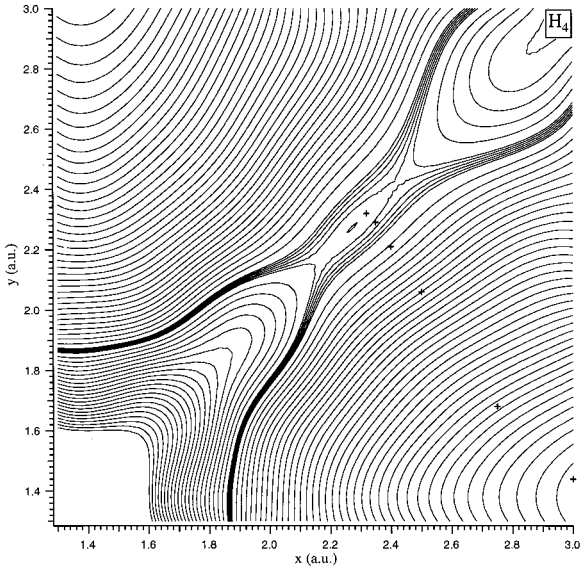

FIG. 1. The two-dimensional potential surface for the reaction H_2+H_2.

being 38 kcal/mol higher than (H_2+2H). Still, due to the formation of (formally) four relatively weak H–H bonds in the TS, it is stable with respect to dissociation to four H atoms, with a corresponding atomization energy of 71 kcal/mol.

The construction of the Kohn–Sham solution from the *ab initio* CI $\rho(\mathbf{r})$ for H_2+H_2 deserves special discussion, due to the strong near-degeneracy correlation effects when the TS state with its high symmetry D_{4h} is approached. On one side of the reaction barrier (for the reagents) $\rho(\mathbf{r})$ is represented with the full-symmetry (in D_{2h}) KS orbital $\psi(a_g)$ and the orbital $\psi(b_{2u})$, which has antibonding character with respect to new bonds (see Fig. 2)

$$\rho(\mathbf{r}) = 2|\psi(a_g)(\mathbf{r})|^2 + 2|\psi(b_{2u})(\mathbf{r})|^2. \tag{3.1}$$

This corresponds to the pure state KS determinant Ψ_{s1}:

$$\Psi_{s1} = \det|\psi(a_g)(\mathbf{r}_1)\alpha\psi(a_g)(\mathbf{r}_1)\beta\psi(b_{2u})(\mathbf{r}_2)\alpha\psi(b_{2u}) \times(\mathbf{r}_2)\beta|. \tag{3.2}$$

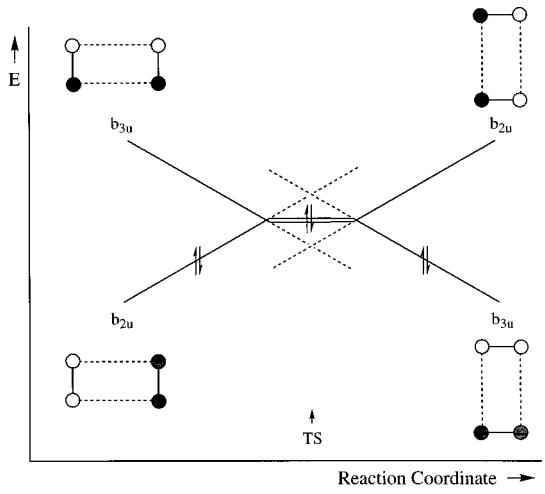

FIG. 2. The orbital correlation diagram for the reaction H_2+H_2.

On the side of the products $\rho(\mathbf{r})$ is represented with $\psi(a_g)$ and the orbital $\psi(b_{3u})$, which has an antibonding character with respect to the old bonds

$$\rho(\mathbf{r})=2|\psi(a_g)(\mathbf{r})|^2+2|\psi(b_{3u})(\mathbf{r})|^2. \tag{3.3}$$

This corresponds to the pure state KS determinant Ψ_{s2}:

$$\Psi_{s2}=\det|\psi(a_g)(\mathbf{r}_1)\alpha\psi(a_g)(\mathbf{r}_1)\beta\psi(b_{3u})(\mathbf{r}_2)\alpha\psi(b_{3u})\times(\mathbf{r}_2)\beta|. \tag{3.4}$$

These two determinants are similar to the HF determinants that would play the main role in the description of the wave function in a CI calculation, which we may denote Ψ_{HF1} and Ψ_{HF2}. When TS is approached the b_{2u} orbital is destabilized and the b_{3u} orbital is stabilized and the mixing of the two determinants in the CI wave function increases. In the TS the b_{2u} and the b_{3u} orbitals become the degenerate e_{u-x}, e_{u-y} pair of orbitals belonging to the E_u irreducible representation of D_{4h}. The wave function will be predominantly the $^1B_{1g}$ CSF

$$\Psi(\mathrm{TS})=\frac{1}{\sqrt{2}}(|e_{u-x}\alpha(1)e_{u-x}\beta(2)|-|e_{u-y}\alpha(1)e_{u-y}\beta(2)|). \tag{3.5}$$

In cases of strong configuration mixing, the KS solution may no longer correspond to a single determinant, but it may be necessary to represent the exact density with an ensemble of KS determinants. The KS potential in that case leads to a degenerate HOMO; see the discussion in Ref. 18 and references therein. This is what we have observed in the present case: as can be seen in Fig. 2, the KS b_{2u} orbital becomes degenerate with the b_{3u} orbital before the TS is reached. If one would continue to occupy the b_{2u} orbital and leave the b_{3u} orbital empty, a non-Aufbau situation would result. This non-Aufbau solution with a hole below the Fermi level is inadmissible in the KS theory, since it corresponds to an excited state of the noninteracting KS system.[35] As a matter of fact, we have observed that it becomes increasingly difficult to generate a local potential that is such that the density of the non-Aufbau determinant is equal to (close to) the exact density.[18] This local potential [which is not the KS potential since its ground state (Aufbau) determinantal density is not the exact density] starts to exhibit strange, unphysical, features. In the neighborhood of the TS, the KS solution that properly reproduces the CI $\rho(\mathbf{r})$ corresponds to a KS potential with degenerate b_{2u} and b_{3u} orbitals. The density is an ensemble density of the noninteracting KS electron system with unequal fractional occupations of the orbitals $\psi(b_{2u})$ and $\psi(b_{3u})$

$$\rho(\mathbf{r})=2|\psi(a_g)(\mathbf{r})|^2+2d|\psi(b_{2u})(\mathbf{r})|^2+2(1-d)|\psi(b_{3u})(\mathbf{r})|^2, \tag{3.6}$$

which corresponds to the KS ensemble density matrix $\hat{M}_s$

$$\hat{M}_s=d|\Psi_{s1}\rangle\langle\Psi_{s1}|+(1-d)|\Psi_{s2}\rangle\langle\Psi_{s2}|. \tag{3.7}$$

Occupation d is determined with the procedure of Ref. 36 from the requirement, that for the KS solution with the density Eq. (3.6) the energies of the orbitals $\psi(b_{2u})$ and $\psi(b_{3u})$ should be equal to each other, thus defining the Fermi level energy ϵ_F

$$\epsilon(\psi(b_{2u}))=\epsilon(\psi(b_{3u}))=\epsilon_F. \tag{3.8}$$

The ground-state KS ensemble Eq. (3.7) does not contain a hole below the Fermi level, as follows from Eqs. (3.6) and (3.8). Since Eq. (3.8) is an exact property of the unique KS solution, which reproduces, ρ, the occupation d is uniquely determined by Eq. (3.8).

TABLE I. Occupations d [Eqs. (3.6) and (3.7)] for the KS and GGA solutions near the transition state at $R=r=2.32$ bohr of the reaction H_2+H_2. At each R the H–H distance r is as indicated by the crosses in Fig. 1. BP and BLYP mean Becke (Ref. 3) exchange and Perdew 1986 (Ref. 1) and LYP (Ref. 2) correlation, respectively. PW means Perdew–Wang 1991 (Refs. 4, 33, 34) exchange and correlation.

R	KS	PW	BP	BLYP
2.32	1.00	1.00	1.00	1.00
2.35	1.36	1.79	1.83	1.80
2.40	1.86	2.00	2.00	2.00
2.50	2.00	2.00	2.00	2.00

In the square TS the D_{4h} symmetry dictates for $\rho(\mathbf{r})$ the form

$$\rho(\mathbf{r})=2|\psi(a_{1g})(\mathbf{r})|^2+|\psi(e_{u-x})(\mathbf{r})|^2+|\psi(e_{u-y})(\mathbf{r})|^2 \tag{3.9}$$

with the singly occupied degenerate orbitals $\psi(e_{u-x})$ and $\psi(e_{e-y})$, which correlate with the orbitals $\psi(b_{3u})$ and $\psi(b_{2u})$, respectively. In this case the KS solution is described by the density matrix $\hat{M}_s$ representing a mixture (ensemble) of the determinants

$$\hat{M}_s=0.5|\Psi_{s3}\rangle\langle\Psi_{s3}|+0.5|\Psi_{s4}\rangle\langle\Psi_{s4}|, \tag{3.10}$$

$$\Psi_{s3}=\det|\psi(a_{1g})(\mathbf{r}_1)\alpha\psi(a_{1g})(\mathbf{r}_1)\beta\psi(e_{u-x})\times(\mathbf{r}_2)\alpha\psi(e_{u-x})(\mathbf{r}_2)\beta|, \tag{3.11}$$

$$\Psi_{s4}=\det|\psi(a_{1g})(\mathbf{r}_1)\alpha\psi(a_{1g})(\mathbf{r}_1)\beta\psi(e_{u-y})\times(\mathbf{r}_2)\alpha\psi(e_{u-y})(\mathbf{r}_2)\beta|. \tag{3.12}$$

This density is identical to the one resulting from a KS $^1B_{1g}$ CSF similar to Eq. (3.5) but built from the KS determinants Ψ_{s3} and Ψ_{s4}. We prefer to use M_s for the representation of the density and for the calculation of the KS energy components for reasons to be discussed below.

Table I presents the occupations d calculated for the points along the reaction path in the neighborhood of the TS. The ensemble KS solution Eq. (3.6) with $d<1$ is found for the segment $2.32\leqslant R\leqslant 2.50$ a.u. (the second column of Table I). For larger intermolecular separations the KS solution is the pure state Eq. (3.2), while with R approaching the TS value $R=2.32$ a.u., the ensemble solution turns to the equi-ensemble Eq. (3.10). It represents a strong nondynamical correlation between the electrons which in the wave function would become manifest as strong mixing of the configurations $(a_g)^2(b_{2u})^2$ and $(a_g)^2(b_{3u})^2$. The self-consistent GGA calculations also produce the ensemble solution Eq. (3.6) near $R=2.32$ a.u. and the equi-ensemble Eq. (3.9) in the TS

(see Table I). In this case occupation d is obtained variationally in the sense that the GGA energy is minimized under the constraint of an *Aufbau* type of electron occupation, i.e., no holes below the Fermi level and fractional occupation for the highest occupied orbitals such that they have equal energies, cf. Eq. (3.8). Note that GGA makes the ensemble region $2.32 \leqslant R \leqslant 2.40$ a.u. smaller compared to the accurate KS solution.

We consider the definition of exchange and correlation energies, and the proper evaluation of these quantities in approximate treatments like LDA and GGA, in case of an interacting electron system for which the corresponding KS system is an ensemble

$$\hat{M}_s = \sum_i d_i |\Psi_{si}\rangle\langle\Psi_{si}|, \tag{3.13}$$

$$\rho(\mathbf{r}) = \sum_i d_i \rho_i(\mathbf{r}). \tag{3.14}$$

The total energy has the form

$$E = \sum_i d_i T_{si} + \int d\mathbf{r}\rho(\mathbf{r}) v_{\text{ext}}(\mathbf{r}) + \frac{1}{2}\int d\mathbf{r}_1\, d\mathbf{r}_2 \frac{\rho(\mathbf{r}_1)\rho(\mathbf{r}_2)}{|\mathbf{r}_1 - \mathbf{r}_2|} + \sum_i d_i E_{xi} + E_c, \tag{3.15}$$

where T_{si} and E_{xi} are the kinetic and exchange energies of the individual one-determinantal component Ψ_{si} of the ensemble

$$T_{si} = \sum_j n_{ij} \int d\mathbf{r}\psi_j^*(\mathbf{r}) \left(-\frac{1}{2}\nabla^2 \right) \psi_j(\mathbf{r}), \tag{3.16}$$

$$E_{xi} = -\frac{1}{4}\sum_j \sum_k n_{ij} n_{ik} \times \int d\mathbf{r}_1\, d\mathbf{r}_2 \frac{\psi_j^*(\mathbf{r}_1)\psi_k(\mathbf{r}_1)\psi_k^*(\mathbf{r}_2)\psi_j(\mathbf{r}_2)}{|\mathbf{r}_1 - \mathbf{r}_2|} \tag{3.17}$$

[the orbital occupations n_{ij} in Eqs. (3.16), (3.17) are either 1 or 0]. Equations (3.15)–(3.17) define the total correlation energy E_c as the difference between the exact total energy and the other KS energy terms which can all be calculated from the KS orbitals. Two comments are in order.

First we note that the difference between the definition of exchange and correlation in the KS theory and the standard quantum chemistry definition[31,37,38] is particularly relevant in cases like the present one. Along the reaction coordinate before and after the TS, there will be strong configuration interaction between $(a_g)^2(b_{2u})^2$ and $(a_g)^2(b_{3u})^2$, leading to a large (nondynamical) correlation energy. In the TS, however, the higher symmetry leads to the restricted Hartree–Fock wave function Eq. (3.5), in which energy lowering due to this mixing is already accounted for, so only dynamical correlation remains. There is therefore a somewhat artificial discontinuity in the conventional correlation energy. As a corrollary, there is similar discontinuity in the RHF exchange energy, since the one-electron energy terms and the Hartree energy will not change strongly at the TS, so the remaining term, which is by definition the exchange energy of the RHF model, will in the TS become much larger (more negative) since it will incorporate the near-degeneracy correlation. In the KS case such a discontinuity does not arise in either the exchange or correlation energy when we use the ensemble representation along the complete reaction coordinate, including the TS point. The crucial point is that we continue to take for the exchange energy a weighted sum of single-determinantal exchange energies. In principle, just at the single point of the D_{4h} symmetry (but nowhere else in the ensemble region) this sum depends on the transformation of the degenerate $e_{u\text{-}x}$ and $e_{u\text{-}y}$ orbitals, which changes the degree of their localization (this problem is a common one for the application of various one-electron methods to high-symmetry states[49]). However, our results show continuity of the energies (3.15) obtained at the high-symmetry point and in its neighborhood where (3.15) is unambigously defined in terms of the canonical KS orbitals. This means that the degenerate orbitals of the TS high-symmetry point we use are the delocalized continuations of the canonical KS orbitals at the adjacent points.

In the second place we note that, in case of an ensemble KS solution, GGAs encounter a problem with the choice of the proper formula for the GGA exchange energy functional. In approximate treatments (LDA, GGA) the exchange energy is not calculated from orbitals but from the density. One can, in the conventional way, insert the total ensemble density Eq. (3.14) into a certain GGA exchange energy functional $E_x^{\text{GGA}}[\rho]$

$$E_x^{\text{GGA}} = E_x^{\text{GGA}}\left[\sum_i d_i \rho_i\right] = \sum_i d_i \int d\mathbf{r}\rho_i(\mathbf{r})\epsilon_x\left(\left[\sum_i d_i\rho_i\right];\mathbf{r}\right). \tag{3.18}$$

Alternatively, in analogy with Eqs. (3.15), (3.17), one can insert the density ρ_i of the individual ensemble components into $E_x^{\text{GGA}}[\rho]$ and sum up the resulting energies over the ensemble

$$E_x^{\text{GGA}}(e) = \sum_i d_i E_x^{\text{GGA}}[\rho_i] = \sum_i d_i \int d\mathbf{r}\rho_i(\mathbf{r})\epsilon_x(\rho_i;\mathbf{r}). \tag{3.19}$$

Evidently, the energies Eqs. (3.18) and (3.19) are not equal to each other. Indeed, each component of Eq. (3.19) represents the exchange interaction of $\rho_i(\mathbf{r})$ with itself, while in Eq. (3.18) this interaction is partially replaced with the interaction with other components $\rho_{j\neq i}$ of the ensemble. The latter interaction is smaller than that of $\rho_i(\mathbf{r})$ with itself, so one can expect that the energy Eq. (3.19) is lower (more negative) than Eq. (3.18). In a different context (the approximate calculation of excited multiplet energies)[39] arguments have been given for the exclusive use of the available approximate exchange functionals for single KS determinants only. Only single determinants will obey with certainty the conditions for the exchange hole that have been used to derive model expressions for the exchange functional. So we use as approximate GGA exchange energy a weighted sum of single-determinantal GGA exchange energies. As will be shown in

TABLE II. CI total energies (a.u.) and the differences between the GGA and CI total energies (kcal/mol) for the path of the reaction H_2+H_2. Column ρ^{CI} is calculated with the KS orbitals for the kinetic energy and ρ^{CI} for all other energy terms. The standard expression Eq. (3.18) for the GGA exchange energy has been used.

			ΔPW		ΔBP		ΔBLYP	
R	r	CI	SCF	ρ_{CI}	SCF	ρ_{CI}	SCF	ρ_{CI}
2.32	2.32	−2.113	15.5	17.7	7.1	9.2	20.4	22.7
2.35	2.29	−2.115	13.9	16.8	5.4	8.3	18.7	21.7
2.40	2.21	−2.127	6.6	10.8	−1.9	2.2	11.4	15.8
2.50	2.06	−2.166	2.1	2.9	−6.4	−5.6	6.6	7.9
2.75	1.68	−2.263	1.3	1.9	−7.0	−6.6	5.1	6.1
3.00	1.44	−2.308	2.8	3.4	−5.4	−5.0	7.7	6.6
4.00	1.41	−2.341	3.7	4.4	−4.7	−4.3	5.5	6.6
5.00	1.40	−2.347	3.8	4.5	−4.8	−4.4	5.2	6.3
10.0	1.40	−2.348	4.0	4.7	−5.4	−5.0	4.7	5.8

the next section, the difference between Eqs. (3.18) and (3.19) is of importance for proper estimation of the H_2+H_2 reaction barrier by GGAs.

IV. COMPARISON OF THE KS AND GGA RESULTS FOR H_2+H_2

Table II compares the total energies calculated along the reaction path of H_2+H_2 by the CI and GGAs. The third column of the table contains the CI total energies (in Hartrees), while other columns contain differences between these CI values and those of the GGA approximations (presented in kcal/mol and the sign defined as $\Delta GGA = E^{GGA} - E^{CI}$.) The columns labeled SCF contain energies from an SCF GGA calculation. The column labeled ρ^{CI} uses the KS orbitals determined from the CI density for the kinetic energy and ρ^{CI} for the electron-nuclear and Hartree energies, and in addition uses ρ^{CI} in the GGA exchange and correlation energies. The standard formula Eq. (3.18) is employed for the exchange energy in both cases. The differences in the kinetic, electron-nuclear and Hartree terms are individually not small, but the summed values are rather close; so are the exchange and correlation energies with ρ^{SCF} and ρ^{CI}, therefore the total energies are close to each other for all functionals and all points considered. All GGAs reproduce the monotonous increase of the CI total energy toward the TS. Compared to the total increase in the CI energy of 0.235 Hartree (147.6 kcal/mol), the ''errors'' are modest, the difference between the SCF and the ρ^{CI} cases being almost an order smaller still.

The CI reaction barrier E^B, the accurate KS contributions to E^B from exchange E_x^B and correlation E_c^B as well as the KS exchange and correlation energies (all in kcal/mol) for the TS and well-separated H_2 molecules at $R=10$ a.u. are presented in the second column of Table III. Note that E_x^B and E_c^B are KS quantities; they are calculated with Eqs. (3.15)–(3.17) using the accurate KS orbitals and the ensemble weights d_i. The exchange brings a large positive contribution $E_x^B = 129$ kcal/mol to E^B, while the correlation makes an appreciable negative contribution $E_c^B = -37.4$ kcal/mol. This may be understood from the exchange (Fermi) and correlation (Coulomb) hole functions $\rho_x(\mathbf{r}_2|\mathbf{r}_1)$ and $\rho_c(\mathbf{r}_2|\mathbf{r}_1)$, from which the exchange energy E_x and the electron–electron potential energy part of the correlation energy, W_c, can be obtained:

$$E_x = \frac{1}{2}\int \frac{\rho(\mathbf{r}_1)\rho_x(\mathbf{r}_2|\mathbf{r}_1)}{|\mathbf{r}_1-\mathbf{r}_2|}\,d\mathbf{r}_1\,d\mathbf{r}_2, \tag{4.1}$$

$$W_c = \frac{1}{2}\int \frac{\rho(\mathbf{r}_1)\rho_c(\mathbf{r}_2|\mathbf{r}_1)}{|\mathbf{r}_1-\mathbf{r}_2|}\,d\mathbf{r}_1\,d\mathbf{r}_2. \tag{4.2}$$

In the separated molecule limit the exchange and correlation in each H_2 molecule are represented with exchange and correlation holes which are localized within a single molecule (the molecule where the reference electron is located). For the exchange hole this can easily be understood from the fact that the exchange hole has approximately the shape of the localized orbital with large amplitude at the reference position.[40,41] The approach to the TS causes delocalization of the exchange hole over all four H atoms. The exchange energy is the weighted average of the exchange energies of the determinants Ψ_{s1} and Ψ_{s2} and in both determinants the exchange hole delocalizes when the interaction between the orbitals on the two monomers becomes strong (orbital localization will be less effective). Delocalization of the exchange hole charge of one electron produces a decrease of the exchange energy (it becomes less negative), hence the observed positive contribution E_x^B to the barrier. The correlation contribution to the barrier is on the contrary negative, since the

TABLE III. Reaction barriers for H_2+H_2 $[E^B = E(R=2.32) - E(R=10)]$ and the exchange and correlation energies for the transition state and $R=10$ a.u. together with the resulting exchange and correlation contributions E_x^B and E_c^B (kcal/mol) to the barrier energy E^B. The entries in the CI/KS column have been obtained from CI energies (for E^B) and from the accurate KS model obtained from the CI density, cf. Eqs. (3.15)–(3.17) for all other energies. The ΔGGA columns contain the differences between the GGA and CI/KS quantities (in kcal/mol), ΔGGA(s) uses the standard formula Eq. (3.18) for the exchange part, ΔGGA(e) the ensemble formula Eq. (3.19). For the correlation energy always $E_c^{GGA}[\rho^C]$ is used.

	CI/KS	ΔPW(s)	ΔPW(e)	ΔBP(s)	ΔBP(e)	ΔBLYP(s)	ΔBLYP(e)
E^B	147.56	13.04	3.21	14.16	3.93	16.85	6.63
E_c(TS)	−88.48	28.44		25.16		38.63	
E_c(10)	−51.06	−6.53		−7.82		2.96	
E_c^B	−37.42	34.97		32.98		35.67	
E_x(TS)	−701.10	−10.71	−20.53	−15.97	−26.20	−15.97	−26.20
E_x(10)	−830.07	11.22	11.22	2.85	2.85	2.85	2.85
E_x^B	128.97	−21.93	−31.75	−18.82	−29.05	−18.82	−29.05

electron correlation effects will be stronger in the weak bonds between the H atoms in the TS than in the strong H–H bonds in each of the two separated monomers. When a reference electron is near one H nucleus, one expects a more strongly localized Coulomb hole surrounding it in the TS state than in an H_2 molecule at equilibrium geometry, cf. Fig. 1 in Ref. 31. The strengthening of the Coulomb correlation in the TS due to the increased nondynamical interatomic (''left–right'') correlation produces the observed negative contribution of the correlation to E^B.

In Table III the differences between the exact KS exchange and correlation contributions and the GGA ones (using ρ^{CI}) are given. The ΔGGA numbers for the total barrier E^B are just the sum of the exchange and correlation contributions, assuming for this comparison that total ''GGA'' energies would be calculated with the KS orbitals for T_s and ρ^{CI} in all other terms, in particular in $E_{xc}^{\mathrm{GGA}}[\rho]$ (cf. column ρ^{CI} in Table II). We note in Table III that the GGA exchange energies have a less repulsive contribution E_x^B than the exact exchange energy of CI/KS. The difference is ca. −20 kcal/mol for the standard GGA energies, Eq. (3.18), and some −10 kcal/mol more for the ensemble expression Eq. (3.19). The GGA correlation energy contribution to the barrier deviates in the opposite (positive) direction from the exact quantity E_c^B. In fact, the difference of +35–+36 kcal/mol is almost as large as the exact E_c^B of −37.4 kcal/mol, implying an almost zero $E_c^B(\mathrm{GGA})$. In order to understand these trends we refer to Refs. 16, 17 where it was established for the case of the dimers Li_2,N_2,F_2 that the exchange GGA functionals with their localized model holes represent effectively just the combination of exchange and molecular nondynamical left–right correlation. This interpretation does not contradict the fact that the GGA exchange functionals (Becke's functional,[3] in particular) are fitted to reproduce only the atomic exchange energies. Indeed, the atomic exchange effects arise from a localized exchange hole, so the approximation that uses atomic results will correspond to a localized hole. In a molecule, however, it is only the combination of exchange and correlation holes, which are individually delocalized, that produces a localized hole that can be modeled as an atomic exchange hole. In their turn, the GGA correlation functionals represent only dynamical correlation, which is also described by a localized hole. Taken together, the GGA exchange and correlation functionals cover all the exchange-correlation effects, which explains the success of GGAs in molecular calculations.

The results for the H_2+H_2 reaction confirm this interpretation of the GGA exchange and correlation. We start our analysis with the correlation functionals. For the separated molecules at $R=10$ a.u., where the correlation energy of each H_2 is close to the energy of the dynamical correlation in the isoelectronic He atom $E_c^{\mathrm{He}}=-0.042$ H$=-26.4$ kcal/mol, the GGA correlation energies E_c^{GGA} for H_2+H_2 are close to the KS value $E_c^{\mathrm{KS}}=-51.1$ kcal/mol [e.g., $E_c(10)$ with PW is at −57.6 kcal/mol only 6.5 kcal/mol lower than E_c^{KS}]. However, while the exact E_c becomes much more negative in the TS (−88.5 kcal/mol), the GGA correlation energies do not follow this trend and stay much closer to the values at large separation [$E_c^{\mathrm{PW}}(\mathrm{TS})$ for instance is −60 kcal/mol, a difference now of +28.4 kcal/mol with E_c^{KS}]. So all GGAs fail to reproduce the strengthening of correlation in the TS due to the nondynamical correlation (note the large positive differences between $E_c^{B(\mathrm{GGA})}$ and E_c^B in Table III). This agrees with the interpretation that the GGA correlation functionals represent only dynamical correlation.

Both exchange GGA functionals considered (Becke and Perdew-Wang) underestimate exchange slightly for the separated molecules, the corresponding error is small (+2.85 kcal/mol) for the Becke functional and it is somewhat larger (+11.2 kcal/mol) for the Perdew-Wang one. However, in the TS they appreciably overestimate exchange with the standard formula Eq. (3.18); the overestimation increases by ca. 10 kcal/mol when the ensemble formula Eq. (3.19) is used. The net effect is a considerable negative deviation of the GGA exchange contribution to the barrier. It is remarkable that this negative deviation compensates the missing effect of the nondynamical correlation in the GGA correlation functionals, so that the GGA errors for the total barrier E^B are considerably smaller than those for the individual components E_c^B and E_x^B. Thus the exchange GGA functionals represent both exchange and, effectively, molecular nondynamical correlation.

This interpretation finds further support from the comparison of the exchange $\epsilon_x(\mathbf{r})$ and exchange-correlation $\epsilon_{xc}(\mathbf{r})$ energy densities constructed for the accurate KS solution with those calculated with GGAs. The energy densities of the LDA are also presented for comparison. In Fig. 3 all energy densities are plotted as functions of the distance x from the bond midpoint along the molecular axis of the H_2 molecule (the H atom is at $x=0.7$ a.u.) separated by 5 a.u. from another H_2 molecule. In spite of the fact that for well-separated molecules both $\epsilon_x(\mathbf{r})$ and $\epsilon_{xc}(\mathbf{r})$ are integrated to nearly the same energies as the GGA functions, their form is very different. This seems to be an exceptional feature of systems H_n with light H atoms, since for systems of heavier elements the KS and GGA energy densities look much more alike.[17] In particular, due to the fact that the KS exchange hole is delocalized over both H atoms of the small H_2 molecule, the corresponding function $\epsilon_x(\mathbf{r})$ has its minimum at the bond midpoint, while $\epsilon_x^{\mathrm{GGA}}(\mathbf{r})$ exhibits a well around the H atom [see Fig. 3(a)]. Note also the clear difference between two GGA exchange energy densities at larger x: $\epsilon_x^B(\mathbf{r})$ has the proper Coulombic asymptotics, so it follows $\epsilon_x(\mathbf{r})$ rather closely in this region, while $\epsilon_x^{\mathrm{PW}}(\mathbf{r})$ decays much faster. The exchange-correlation function $\epsilon_{xc}(\mathbf{r})$ has a very shallow descent when going from the bond midpoint to the H atom [see Fig. 3(b)]; still the overall picture is similar to that for the exchange-only functions, since in this case the exchange clearly dominates over the correlation. All approximate functions are appreciably more negative than $\epsilon_x(\mathbf{r})$ and $\epsilon_{xc}(\mathbf{r})$ around the nucleus and they are higher at larger x, so that the good agreement between the KS and GGA energies emerges as a result of the cancellation of the GGA local errors in these regions.

Note that the comparison of the GGA energy densities with the KS ones can be criticized,[42] because (1) the GGA and KS functions might have different definitions due to the nonuniqueness of the energy density and (2) depending on its

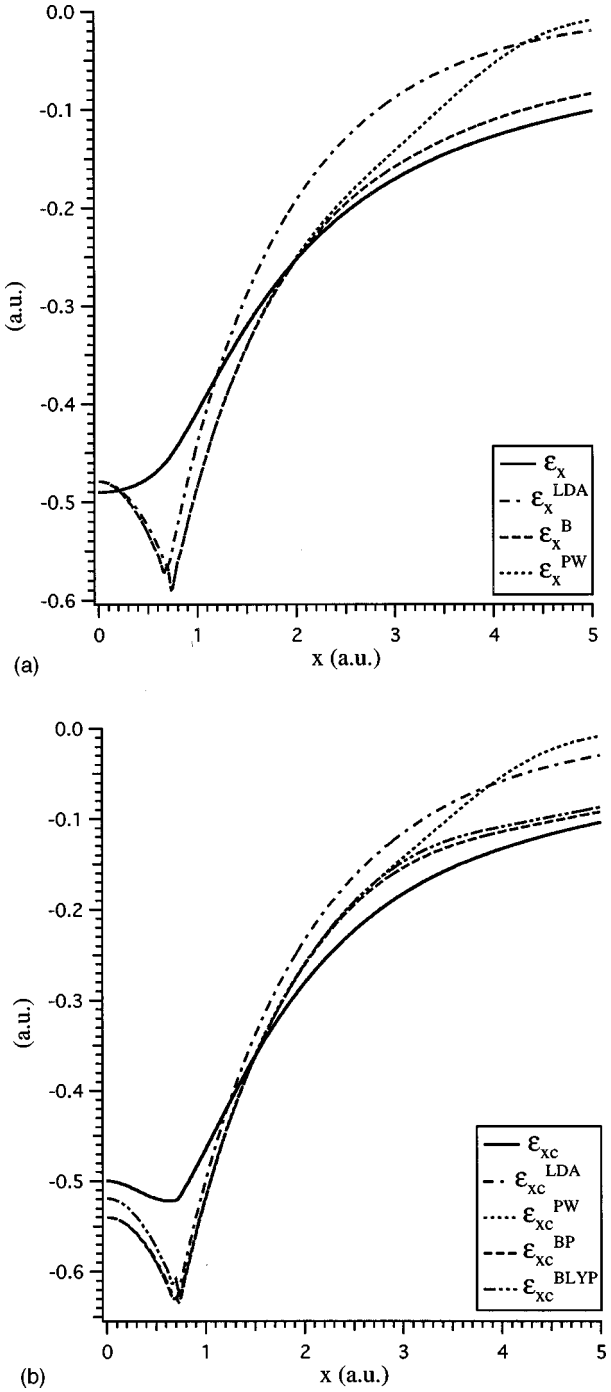

FIG. 3. The Kohn–Sham and GGA energy densities for the H_2 unit of the H_2+H_2 at $R=5$ a.u. (a) Exchange energy densities and (b) exchange-correlation energy densities.

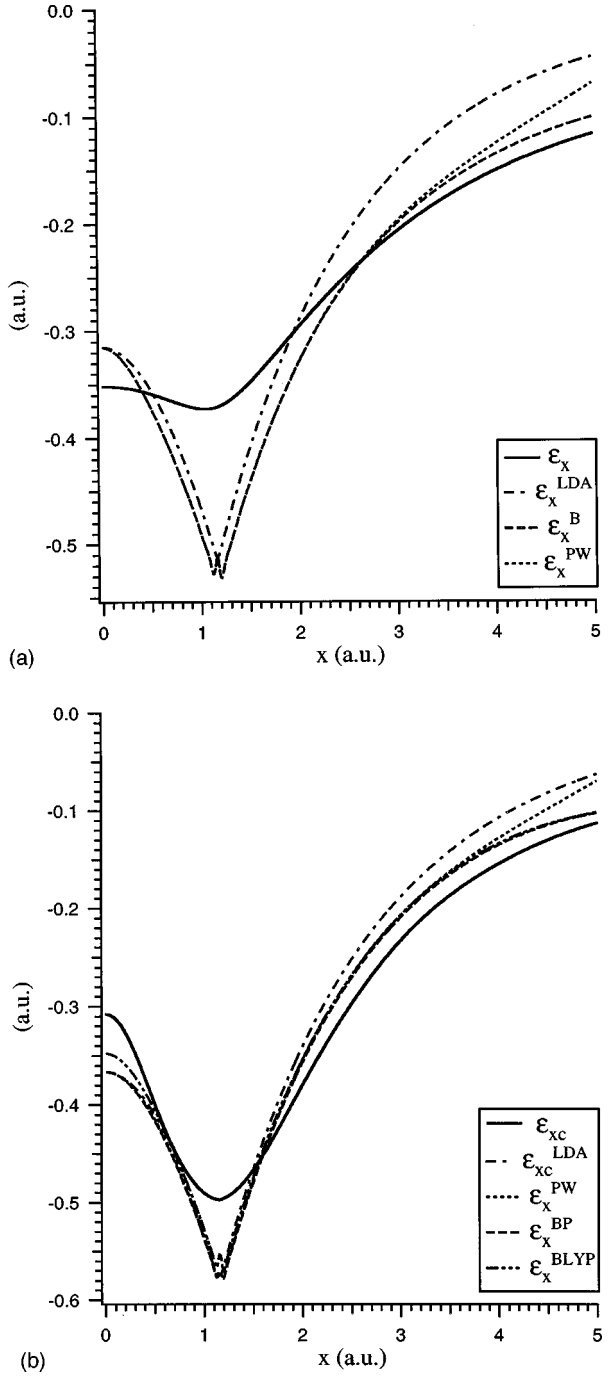

FIG. 4. The Kohn–Sham and GGA energy densities for the transition state of the H_2+H_2 reaction. (a) Exchange energy densities and (b) exchange-correlation energy densities.

actual structure, a certain GGA energy density can be transformed within the procedure of partial integration, which preserves the resulting energy, but changes the form of the energy density function. These reasons, however, cannot explain the observed differences between the KS and GGA functions. It is the exchange that dictates the form of the curves in Fig. 3, but both GGA and KS exchange energy densities are based on the same definition Eq. (2.5). Furthermore, the GGA exchange energy densities behave like the LDA one and, indeed, they contain the LDA part. The latter, however, is a trivial function $c\rho^{1/3}$.

In Fig. 4 the GGA and KS energy densities for the TS are also plotted as functions of the distance x from the midpoint of the bond between two H atoms with the H atom placed at $x=1.16$ a.u. Due to the delocalization of the exchange hole over all four H atoms, the KS $\epsilon_x(\mathbf{r})$ in Fig. 4(a) remains a shallow function in the bonding region. Here, the difference between $\epsilon_x(\mathbf{r})$ and the corresponding GGA functions becomes even larger than in Fig. 3(a), which reflects the abovementioned effective inclusion of the strong nondynamical correlation in the TS into the GGA exchange functionals. Note the pronounced bond midpoint peak of both

LDA and GGA functions, which brings them to higher energies than $\epsilon_x(\mathbf{r})$. Remarkably, with the inclusion of the nondynamical correlation at the KS level, the form of the total exchange-correlation KS function $\epsilon_{xc}(\mathbf{r})$ becomes much closer to that of the corresponding GGA functions [see Fig. 4(b)]. Now, $\epsilon_{xc}(\mathbf{r})$ possesses the same pronounced peak as the GGA exchange-only functions, which indicates that the GGA exchange functionals attempt to simulate not only the effect of the nondynamical correlation on the integrated energies, but also its local influence on the form of the energy density functions.

The most important result of this section is the good performance of the ensemble formula Eq. (3.19) for the GGA exchange energy. Indeed, the GGA reaction barriers calculated with the standard formula Eq. (3.18) are appreciably higher than the CI one (by 13–17 kcal/mol, see Table III). However, the employment of the ensemble formula improves considerably the performance of the GGAs. In particular, the barrier error reduces to 3.2 kcal/mol for the PW functional and to 3.9 kcal/mol for BP, while BLYP produces a somewhat larger error of 6.6 kcal/mol. To improve the quality of the reaction barriers calculated with approximate DFT methods, it was proposed in the literature[8] to use the hybrid schemes,[43,44] in which standard LDA and GGA exchange-correlation functionals are combined with the KS/HF exchange functional built from the LDA orbitals. It has also been proposed[5,45] to improve density functional results for TS barriers by the use of the self-interaction correction (SIC),[46] where a part of the LDA/GGA exchange-correlation functional is replaced with minus the sum of the exact self-interaction terms for the occupied orbitals. In its effect SIC is, to some extent, similar to the hybrid schemes, since the inserted self-interaction terms constitute a major part of the KS/HF exchange. Both schemes can help in cases where the standard GGA methods underestimate barriers (as in the case of the $H+H_2$ reaction studied in the next section), otherwise the use of the hybrid schemes or SIC may worsen the results as well. As one can see from Table III, in the case of H_2+H_2 any mixture of the KS exchange with the GGA exchange-correlation functional can only increase the already too high barrier and therefore worsen the agreement with the accurate CI value.

Based on the comparison between GGAs and the accurate KS/CI performed in this section, we recommend to use the exchange energy expression Eq. (3.19) in cases of symmetry (or near-symmetry) degeneracy as well as in cases of the accidental degeneracy[18] when GGA produces an ensemble KS solution Eq. (3.7) with fractional occupations of the degenerate KS orbitals at the Fermi level.

V. COMPARISON OF THE KS AND GGA RESULTS FOR $H+H_2$

Table IV compares the total CI energies calculated along the collinear reaction path of the hydrogen abstraction reaction $H+H_2$ with GGA energies. It is organized in the same manner as Table II—the CI energies are presented in Hartrees and the differences between the GGA and CI energies are presented in kcal/mol. The energies are given for a number of distances R between the incoming H atom and the neighboring atom of the H_2 molecule; the bond distance r of the latter is optimized for each R. In the transition state H_3 with $R=r=1.76$ a.u. the H–H bond of the isolated H_2 molecule is replaced with a three-center bond, which is represented with the full-symmetry KS orbital $\psi(1\sigma_g)$, while the unpaired electron occupies the nonbonding orbital $\psi(1\sigma_u)$, which has a node on the central H atom. The bonding in the TS is only slightly weaker than in H_2, so that the CI energy of $H+H_2$ slowly increases toward TS and the reaction barrier is only 9.64 kcal/mol. Again, the GGA energies calculated self-consistently and with the CI $\rho(\mathbf{r})$ and corresponding KS orbitals are close to each other, which allows us to concentrate our analysis on the latter results.

TABLE IV. CI total energies (a.u.) and the differences between the GGA and CI total energies (kcal/mol) for the path of the reaction $H+H_2$.

			ΔPW		ΔBP		ΔBLYP	
R	r	CI	SCF	ρ_{CI}	SCF	ρ_{CI}	SCF	ρ_{CI}
1.76	1.76	−1.659	−5.2	−3.3	−11.5	−9.9	−2.9	−0.8
1.80	1.71	−1.659	−5.1	−3.3	−11.5	−9.9	−2.9	−0.8
1.90	1.62	−1.659	−4.8	−3.0	−11.1	−9.5	−2.6	−0.4
2.00	1.57	−1.660	−4.4	−2.5	−10.6	−8.9	−2.2	0.0
2.25	1.49	−1.662	−3.1	−1.1	−9.1	−7.3	−0.9	1.3
2.50	1.45	−1.665	−2.0	0.1	−7.6	−5.9	0.3	2.5
3.00	1.42	−1.669	−0.3	1.4	−5.3	−3.9	2.1	3.9
4.00	1.41	−1.673	0.9	2.0	−3.2	−2.4	3.6	4.8
5.00	1.40	−1.674	1.09	2.0	−2.6	−2.0	3.9	5.0

Table V is organized in the same way as Table III. It presents in the first row the CI reaction barrier E^B, and the deviations of the GGA barrier heights from the CI barrier. The deviations are all negative and appreciable, i.e., the GGA barriers are 50% and more reduced compared to the CI barrier. Table V also lists in the CI/KS column the accurate KS contributions to E^B from exchange E_x^B and correlation E_c^B (all in kcal/mol), as well as the KS exchange and correlation energies for the TS and for $R=5$ a.u. from which the values for the corresponding contributions to the barrier height are derived. As in the case of the H_2+H_2 TS of the previous section, the KS exchange brings a large positive contribution $E_x^B=29.7$ kcal/mol, while the correlation makes an appreciable negative contribution $E_c^B=-14.5$ kcal/mol. For the exchange this can be explained again as a result of the delocalization of the unit charge of the exchange hole in the TS,

TABLE V. Reaction barriers E^B for the reaction $H+H_2$ with the exchange and correlation contribution (kcal/mol), the exchange and correlation energies for the transition state and $R=5$ a.u. calculated with CI/KS, and the differences between the GGA and CI/KS quantities (in kcal/mol) (see also caption to Table II).

	CI/KS	ΔPW	ΔBP	ΔBLYP
E^B	9.64	−5.4	−8.0	−5.8
E_c(TS)	−40.79	−0.50	−2.08	7.04
E_c(5)	−26.32	−6.71	−5.11	1.85
E_c^B	−14.47	6.2	3.0	5.2
E_x(TS)	−581.31	−2.85	−7.86	−7.86
E_x(5)	−611.01	8.72	3.15	3.15
E_x^B	29.70	−11.6	−11.0	−11.0

which leads to a decrease of the exchange energy. As for the negative correlation contribution to the barrier, the weaker bond in the TS leads to a larger (more negative) correlation effect in the TS due to the stronger nondynamical left–right correlation.

The other columns of Table V exhibit the differences of the GGA quantities from the corresponding CI/KS ones (sign of ΔGGA quantities defined as $E^{\mathrm{GGA}}-E^{\mathrm{CI/KS}}$). The differences for the separate energy components—exchange, correlation—allow us to analyze what causes the GGA error in the barrier height (first row of Table V). We note that the GGA exchange energy contribution to the barrier is ca. 11 kcal/mol less positive than the KS one. Again, this is to be attributed to the fact that GGA exchange incorporates the nondynamical correlation effect. Indeed, the differences $E_x^B(\mathrm{PW})-E_x^B=-11.6$ kcal/mol and $E_x^B(B)-E_x^B=-11.0$ kcal/mol between the GGA and KS exchange contributions to the barrier approach the KS result -14.5 for E_c^B, which of course also contains a small dynamical correlation contribution. This is analogous to to the H_2+H_2 case, where the $E_x^B(\mathrm{GGA})$ differed ca. -30 kcal/mol from the KS exchange barrier, to be compared to the KS result of -37.4 kcal/mol for E_c^B in that case.

The performance of the GGA correlation functionals in this case, however, differs from that for H_2+H_2. In the latter case the GGA correlation energies yield only small negative $E_c^B(\mathrm{GGA})$ of a few kcal/mol (the ΔGGA numbers for E_c^B are ca. $+35$ kcal/mol, canceling most of the -37.4 kcal/mol for E_c^B). This is consistent with the assumption that the negative E_c^B is mostly a nondynamical correlation effect, whereas the GGA correlation functionals only represent the dynamical correlation, which differs little between the TS and separated systems. However, for the H_3 E_c^B the ΔGGA numbers, although being positive, by no means cancel the KS E_c^B. In fact, the GGAs bring appreciable (compared to the height of the barrier) negative contributions to the barrier $E_c^B(\mathrm{GGA})=E_c^B+\Delta(\mathrm{GGA})$, i.e.; $E_c^B(\mathrm{PW91})=-8.3$ kcal/mol, $E_c^B(\mathrm{P86})=-11.5$ kcal/mol and $E_c^B(\mathrm{LYP})=-9.3$ kcal/mol. If the GGAs for correlation do not represent the nondynamical correlation in the TS (which causes the negative KS E_c^B of -14.5 kcal/mol), but do describe dynamical correlation, they apparently overestimate the dynamical correlation in the H_3 TS. In the TS the lack of nondynamical correlation in the GGAs for correlation should cause appreciable positive ΔGGA values (as is the case in the H_2+H_2 TS, see Table III), but the correlation energies $E_c(\mathrm{TS})$ of the GGA PW91 and P86 functionals are similar to [actually 0.5–2 kcal/mol larger (more negative) than] the KS one, and only the LYP energy is somewhat smaller, but it is also smaller for the separated H and H_2 (see Table V).

Thus, a possible reason of the too low GGA barriers for the hydrogen abstraction reactions is the overestimation by the GGA correlation functionals of the dynamical correlation in open-shell systems (such as the H_3 TS), for which a typical absolute value of the local polarization $\zeta(\mathbf{r})=[\rho^{\uparrow}(\mathbf{r})-\rho^{\downarrow}(\mathbf{r})]/\rho(\mathbf{r})$ is in between 0 and 1. By construction, all the GGA correlation functionals considered yield only a small artificial correlation energy for the separated H atom with $\zeta(\mathbf{r})=1$. In particular, it equals 2 kcal/mol for P86,[1] it is 0.07 kcal/mol for PW91,[34] and the LYP functional by construction[2] has the correct zero correlation energy for H. However, the GGA correlation functionals may well overestimate slightly the dynamical correlation for the intermediate polarizations $0<|\zeta(\mathbf{r})|<1$. This appears to be the case for the H_3 TS where the unpaired electron is localized on the terminal H atoms, so that for these atoms $|\zeta(\mathbf{r})|$ is in between 0 and 1. This conclusion is supported by the fact that, generally, GGAs tend to underestimate barriers of radical abstraction reactions in open-shell systems. Based on the comparison between GGAs and the accurate KS/CI performed in this section, we recommend to modify the ζ-dependence of the approximate correlation functionals in order to reduce the correlation for the intermediate ζ values and, as a result, to increase the barriers calculated for radical abstraction reactions.

It is also possible to try to correct the GGA results straightforwardly by trying to develop an exchange functional that gives results close to the exact (KS) exchange, and a correlation functional that agrees closely with the KS E_c, both in the TS and in the separated systems. It has in fact been proposed in the literature[5,8,45] to improve the calculated barriers by using the hybrid ''KS exchange+GGA/LDA exchange-correlation'' schemes or the self-interaction correction (SIC). Of course developing functionals for the exact KS exchange and correlation are perfectly valid and would, if such functionals can be found, provide the desired solution to the GGA error for the barrier. In fact, such a scheme would, by construction, also provide an exact description of the simplest molecular open-shell system H_2^+, for which the LDA and GGA exchange functionals make a large error compared to the exact (KS) exchange at long bond distance. Recently, this system was discussed in the literature in connection with the failure of GGA for weak three-electron two-center bonds.[47] We here propose an alternative remedy, which is based on our observation[16,17] that the present GGA ''exchange'' functionals do not in fact describe ''exact exchange'' very well, but describe the exchange plus nondynamical correlation quite accurately. Since this also appears to hold in the $H+H_2$ transition state, that leaves the GGA ''correlation'' functional as the only functional to be corrected for its overestimation of the dynamical correlation in cases of intermediate spin polarization.

In Figs. 5 and 6 the exchange $\epsilon_x(\mathbf{r})$ and exchange-correlation $\epsilon_{xc}(\mathbf{r})$ energy densities constructed for the accurate KS solution are compared with those calculated with GGAs and LDA. All energy densities are plotted along the main axis of the reaction system H_3 with the origin placed at the central H atom. In particular, Fig. 5(a), 5(b) shows the H atom and H_2 molecule separated at $R=5$ a.u. Evidently, their H_2 portions display the same picture as that in Fig. 3(a), 3(b) for the separated H_2 fragment of the H_2+H_2 system discussed in the previous section. The separated H atom is represented with a well, which describes the excluded self-interaction of the $1s$-electron. For both H and H_2 all GGA functions are too low around the nuclei and too high at larger electron-nuclear distances.

Figure 6 shows the H_3 TS. The shallow form of the KS $\epsilon_x(\mathbf{r})$ reflects delocalization of the exchange hole over all

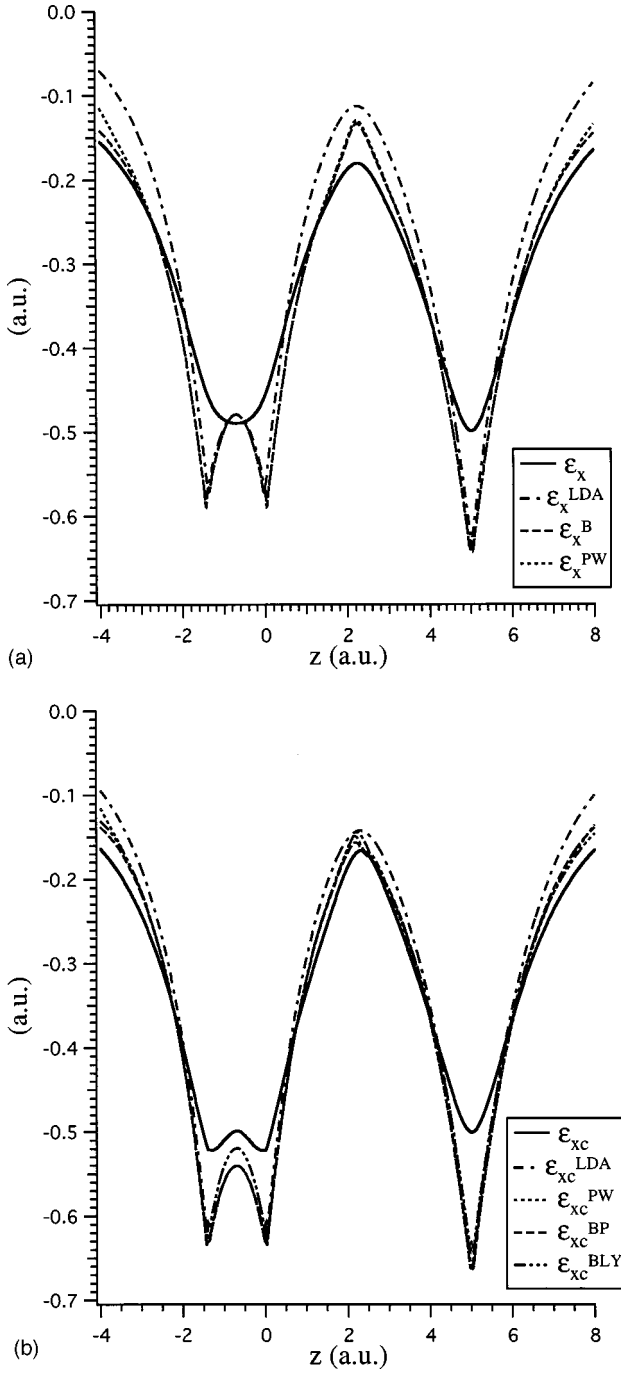

FIG. 5. The Kohn–Sham and GGA energy densities for the $H+H_2$ at $R=5$ a.u. (a) Exchange energy densities and (b) exchange-correlation energy densities.

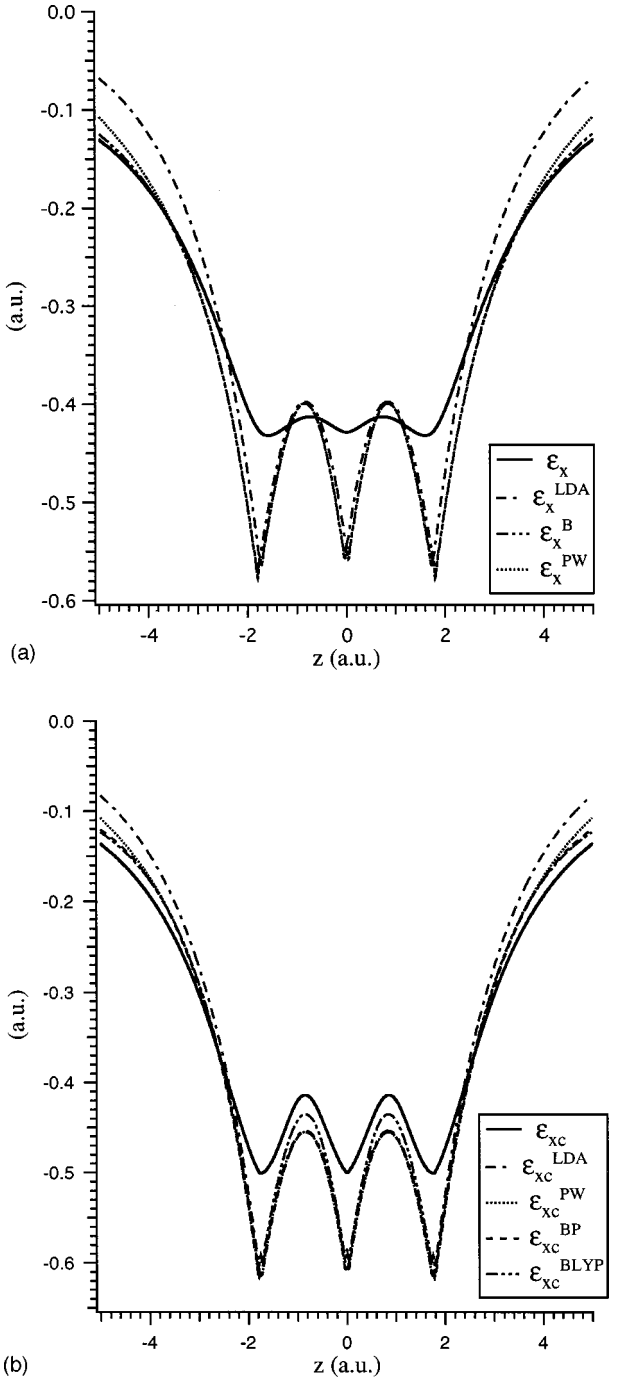

FIG. 6. The Kohn–Sham and GGA energy densities for the transition state of the $H+H_2$ reaction. (a) Exchange energy densities and (b) exchange-correlation energy densities.

three H atoms, while the GGA exchange functionals exhibit rather sharp wells around all H atoms. These wells of course persist in the ϵ_{xc}^{GGA} functions in Fig. 6(b), becoming actually slightly deeper than in ϵ_{xc}^{GGA}. As in the case of H_2+H_2, the inclusion of the nondynamical left–right correlation at the KS level brings more pronounced wells around the nuclei and peaks in the bond midpoint regions in $\epsilon_{xc}(\mathbf{r})$, which therefore is closer to $\epsilon_{xc}^{GGA}(\mathbf{r})$. Still, the corresponding local differences are large, with $\epsilon_{xc}^{GGA}(\mathbf{r})$ being too low in the whole interior region of the H_3 TS and too high for $|z|>2.4$ a.u. In spite of these local differences, a remarkably good agreement between the integrated KS and GGA exchange-correlation energies (cf. Table V) emerges as a result of cancellation of the differences between the corresponding energy densities.

VI. CONCLUSIONS

In this paper the KS solution has been constructed from the CI density and the KS exchange E_x and correlation E_c energies; as well, the corresponding exchange $\epsilon_x(\mathbf{r})$ and exchange-correlation $\epsilon_{xc}(\mathbf{r})$ energy densities have been obtained for the simplest hydrogen abstraction reaction $H+H_2$

and the four-center exchange reaction H_2+H_2. The KS/CI quantities and functions have been compared with those of the standard GGAs. The comparison corroborates our earlier finding[16,17] that within GGA the exchange functional represents both exchange and molecular nondynamical left–right correlation, while the correlation functional represents only the dynamical part of the correlation. This role of the GGA exchange functional is especially important for the transition states of the reactions where the left–right correlation is enhanced.

The standard GGAs tend to underestimate the barrier height for the reaction $H+H_2$ and to overestimate it for the reaction H_2+H_2. For the latter reaction the Kohn–Sham orbital symmetry degeneracy in the TS is represented with equi-ensemble KS solutions for both accurate KS/CI and GGA, while near the TS ensemble solutions with unequal occupations of the degenerate orbitals have been obtained. In the general case of the GGA ensemble solution it has been proposed to use a corresponding ensemble formula for the GGA exchange functional. Application of this formula to the H_2+H_2 reaction reduces appreciably the reaction barriers calculated with GGAs and leads to a much better agreement with the accurate value.

The too low GGA barriers for the $H+H_2$ reaction have been attributed to the overestimation of the dynamical correlation in the TS by the GGA correlation functionals. In order to correct this error and, in general, the too low GGA barriers for radical abstraction reactions, it has been recommended to modify the dependence of the approximate correlation functionals on the local polarization ζ with the purpose to reduce the correlation for intermediate ζ values, which are expected to characterize transition states of these reactions. It has been proposed in the literature[5,8,45] to improve the calculated barriers by using the hybrid KS ''exchange+GGA/LDA exchange-correlation'' schemes or the self-interaction correction (SIC). However, this approach, which will increase the barrier, would not work in cases where the barrier is already too high, and we have identified the reaction H_2+H_2 considered in Sec. IV as such a case. So, rather than trying to correct the GGA exchange so as to bring it closer to the exact (KS) exchange, we consider the GGA ''exchange'' functional as an approximation to exchange plus nondynamical correlation. This is based on our earlier observation[16,17] that the GGA ''exchange'' in fact does provide a good approximation to exchange plus nondynamical correlation. It is then the overestimation of dynamical correlation by the GGA ''correlation'' functionals in cases of intermediate spin-polarization that has to be corrected. The recommendations developed in this paper do not interfere with each other. The ensemble formula for the exchange energy which is applicable in the H_2+H_2 case and other cases[48] can be naturally incorporated into existing DFT models and improvements using the ζ-dependence of approximate correlation functionals, which are relevant for radical reactions like $H+H_2$, can be developed independently.

[1] J. P. Perdew, Phys. Rev. B **33**, 8822 (1986) [Erratum: Phys. Rev. B **34**, 7406 (1986)].
[2] C. Lee, W. Yang, and R. G. Parr, Phys. Rev. B **37**, 785 (1988).
[3] A. Becke, Phys. Rev. A **38**, 3098 (1988).
[4] J. P. Perdew, K. Burke, and Y. Wang, Phys. Rev. B **54**, 16533 (1996).
[5] B. G. Johnson, C. A. Gonzales, P. M. W. Gill, and J. A. Pople, Chem. Phys. Lett. **221**, 100 (1994).
[6] D. Porezag and M. R. Pederson, J. Chem. Phys. **102**, 9345 (1995).
[7] H. Chermette, H. Razafinjanahary, and L. Carrion, J. Chem. Phys. **107**, 10643 (1997).
[8] S. Skokov and R. A. Wheeler, Chem. Phys. Lett. **271**, 251 (1997).
[9] C. O. Almbladh and A. C. Pedroza, Phys. Rev. A **29**, 2322 (1984).
[10] F. Aryasetiawan and M. J. Stott, Phys. Rev. B **34**, 4401 (1986).
[11] Q. Zhao, R. C. Morrison, and R. G. Parr, Phys. Rev. A **50**, 2138 (1994).
[12] R. C. Morrison and Q. Zhao, Phys. Rev. A **51**, 1980 (1995).
[13] M. A. Buijse, E. J. Baerends, and J. G. Snijders, Phys. Rev. A **40**, 4190–4202 (1989).
[14] O. V. Gritsenko, R. van Leeuwen, and E. J. Baerends, Phys. Rev. A **52**, 1870 (1995).
[15] O. V. Gritsenko, R. van Leeuwen, and E. J. Baerends, J. Chem. Phys. **104**, 8535 (1996).
[16] O. V. Gritsenko, P. R. T. Schipper, and E. J. Baerends, J. Chem. Phys. **107**, 5007 (1997).
[17] P. R. T. Schipper, O. V. Gritsenko, and E. J. Baerends, Phys. Rev. A **57**, 1729 (1998).
[18] P. R. T. Schipper, O. V. Gritsenko, and E. J. Baerrends, Theor. Chem. Acc. **99**, 329 (1998).
[19] V. E. Ingamells and N. C. Handy, Chem. Phys. Lett. **248**, 373 (1996).
[20] D. J. Tozer, V. E. Ingamells, and N. C. Handy, J. Chem. Phys. **105**, 9200 (1996).
[21] P. Süle, O. V. Gritsenko, A. Nagy, and E. J. Baerends, J. Chem. Phys. **103**, 10085–10094 (1995).
[22] O. V. Gritsenko, R. van Leeuwen, and E. J. Baerends, Int. J. Quantum Chem. **60**, 1375 (1996).
[23] P. R. T. Schipper, O. V. Gritsenko, and E. J. Baerends, Theor. Chem. Acc. **98**, 16 (1997).
[24] J. C. Slater, *Quantum Theory of Molecules and Solids, Vol. 4* (McGraw-Hill, New York, 1974).
[25] S. H. Vosko, L. Wilk, and M. Nusair, Can. J. Phys. **58**, 1200 (1980).
[26] R. van Leeuwen and E. J. Baerends, Phys. Rev. A **49**, 2421–2431 (1994).
[27] V. R. Saunders and J. H. van Lenthe, Mol. Phys. **48**, 923 (1983).
[28] T. H. Dunning, J. Chem. Phys. **90**, 1007 (1988).
[29] W. R. Schulz and D. J. LeRoy, J. Chem. Phys. **42**, 3869 (1965).
[30] D. L. Diedrich and J. B. Anderson, Science **258**, 786 (1992).
[31] E. J. Baerends and O. V. Gritsenko, J. Phys. Chem. **101**, 5383 (1997).
[32] M. A. Buijse, Thesis, Vrije Universiteit, 1991.
[33] J. P. Perdew, in *Electronic Structure of Solids*, edited by P. Ziesche and H. Eschrig (Akademie, Berlin, 1991), pp. 11–20.
[34] J. P. Perdew, J. A. Chevary, S. H. Vosko, K. A. Jackson, M. R. Pederson, D. J. Singh, and C. Fiolhais, Phys. Rev. B **46**, 6671 (1992).
[35] M. Levy and J. P. Perdew, Phys. Rev. A **32**, 2010 (1985).
[36] F. W. Averill and G. S. Painter, Phys. Rev. B **46**, 2498 (1992).
[37] E. J. Baerends, O. V. Gritsenko, and R. van Leeuwen, in *Chemical Applications of Density Functional Theory*, Vol. 629, edited by B. B. Laird, R. B. Ross, and T. Ziegler (American Chemical Society, Washington, DC, 1996), pp. 20–41.
[38] E. K. U. Gross, M. Petersilka, and T. Grabo, in *Chemical Applications of Density Functional Theory*, Vol. 629, edited by B. B. Laird, R. B. Ross, and T. Ziegler (American Chemical Society, Washington, DC, 1996), pp. 42–53.
[39] T. Ziegler, A. Rauk, and E. J. Baerends, Theor. Chim. Acta **43**, 261 (1977).
[40] W. L. Luken, Int. J. Quantum Chem. **22**, 889 (1982).
[41] M. A. Buijse and E. J. Baerends, in *Electronic Density Functional Theory of Molecules, Clusters and Solids*, edited by D. E. Ellis (Kluwer Academic Publishers, Dordrecht, 1995), pp. 1–46.
[42] J. P. Perdew, K. Burke, and M. Ernzerhof, in *Chemical Applications of Density Functional Theory*, Vol. 629, edited by B. B. Laird, R. B. Ross, and T. Ziegler (American Chemical Society, Washington, DC, 1996), pp. 453–462.
[43] A. D. Becke, J. Chem. Phys. **98**, 1372 (1993).
[44] A. D. Becke, J. Chem. Phys. **98**, 5648 (1993).
[45] G. I. Csonka and B. G. Johnson, Theor. Chem. Acc. **99**, 158 (1998).
[46] J. P. Perdew and A. Zunger, Phys. Rev. B **23**, 5048 (1981).
[47] M. Sodupe, J. Bertran, L. Rodriguez-Santiago, and E. J. Baerends, J. Phys. Chem. **103**, 166 (1999).
[48] S. G. Wang and W. H. E. Schwarz, J. Chem. Phys. **105**, 4641 (1996).
[49] M. Filatov and S. Shaik, J. Chem. Phys. **110**, 116 (1999).